

Magnetic Cobalt Nanowire Thin Films

Hongmei Luo, Donghai Wang, Jibao He, and Yunfeng Lu*

Department of Chemical and Biomolecular Engineering, Tulane University, New Orleans, Louisiana 70118

Received: September 30, 2004; In Final Form: November 22, 2004

Two-dimensional (2D) and three-dimensional (3D) magnetic cobalt nanowire thin films with tunable 3–10 nm wire diameters have been electrodeposited using mesoporous silica templates containing 2D hexagonal or 3D cubic pore channels. As compared to bulk cobalt films, the cobalt nanowire thin films exhibit enhanced coercivities and controllable magnetic anisotropy through tuning of the mesostructure and dimension of the nanowires. Such novel magnetic nanowire thin films may provide a new platform for high-density information storage applications.

Introduction

The rapid development of information technology calls for high-density information storage media. A possible strategy toward this challenge is to reduce magnetic domain sizes by using low-dimensional magnetic materials such as magnetic nanoparticles, nanorods, or nanowires.^{1–3} It is expected that patterned magnetic nanowire arrays may provide a recording density on the order of 100 Gb/inch².⁴ However, as the grain size decreases, originally ferromagnetic particles may become superparamagnetic and can no longer be used as the magnetic storage media. For example, two-dimensional (2D) or three-dimensional (3D) superlattices assembled from 2 to 11 nm cobalt nanoparticles showed superparamagnetic behavior at room temperature.^{5–8} Such a superparamagnetic behavior is due to the overcoming of magnetic anisotropy by thermal energy that randomizes the magnetization orientation. As compared to magnetic nanoparticles, although nanowires have small wire diameters, they may still show ferromagnetism at room temperature because of the volume effect and enhanced magnetic shape anisotropy.^{1–3,9} Fabrication of magnetic nanowire-based devices therefore holds great promise for future high-density information storage.

Various magnetic nanowires have been synthesized using methods such as electron beam lithography, X-ray lithography, scanning probe lithography, step growth methods, nano-imprint, and templating approach.^{3,10} Among these methods, the template-assisted electrodeposition is particularly attractive due to its simplicity, low-cost, and high yield. It provides an efficient route for fabricating isolated ferromagnetic nanowire columns with small diameters that are determined by the pore diameter of the templates.^{11,12} To date, arrays of ferromagnetic metals (e.g., Co, Ni, and Fe), alloys (e.g., NiFeCo and CoPt), and multilayer (e.g., Cu/Co, Cu/Ni) nanowires have been prepared using porous polycarbonate or anodized aluminum oxide (AAO) membranes as templates.^{1–3,11–28} It has been demonstrated that a smaller nanowire diameter often enhances the coercivity, a key factor for data storage. However, these common templates often contain pore diameters greater than 30 nm, limiting the synthesis of nanowires with smaller diameters.

This research reports the electrochemical deposition of 2D and 3D magnetic nanowires with smaller wire diameters (e.g.,

3–10 nm) using mesoporous silica films as templates. Mesoporous silica thin films can be readily prepared on conductive substrates through cooperative assembly of silicate and surfactant using a simple sol–gel dip-coating or spin-coating process.²⁹ The pore diameters are unimodally controllable from 2 to 20 nm, and these pore channels are organized into 2D hexagonal, 3D cubic, or other mesostructures.^{29,30} Furthermore, it may be possible to align the pore channels parallel or perpendicular to the substrate.³¹ These unique features allow precise controls over nanowire diameters and their mesoscale arrangements.^{32–37} Although nanowires with diameters of 3–7 nm have been synthesized using porous AAO, carbon nanotubes, or tobacco mosaic virus as templates, there are no reports on their magnetic properties.^{18,27,28,38,39}

Experimental Section

Sample Preparation. The mesoporous silica templates were prepared by spin-coating the silicate/surfactant sols on ITO-glass substrates. The surfactants used included Pluronic P123 (EO₂₀PO₇₀EO₂₀, EO = –CH₂CH₂O–, PO = –CH₂(CH₃)–CHO–), CTAB (cetyltrimethylammonium bromide, CH₃–(CH₂)₁₅N⁺(CH₃)₃Br[–]), and Brij-58 (C₁₆H₃₃(OCH₂CH₂)₂₀OH). The sols were prepared by mixing 1 g of tetraethoxysilane (TEOS, 98%), 0.2–0.3 g of surfactant, 0.4 g of 0.1 N HCl, and 4.2 g of ethanol at room temperature for 30 min. Spin-coated thin films were calcined at 400 °C for 1 h in air to remove the surfactant, resulting in mesoporous thin films with an average thickness of 200 nm. Mesoporous silica thin films with 2D hexagonal pore channels were prepared using CTAB and P123 as the pore-directing agents. Mesoporous silica thin films with 3D cubic pore channels were prepared using Brij-58 as the pore-directing agent. Electrochemical deposition was performed in a standard three-electrode glass cell consisting of a mesoporous silica-coated ITO-glass cathode, a Pt gauze anode, and a Ag/AgCl reference electrode. The electrolyte contained 20 v% of methanol, Co salt (1.3 M CoSO₄·5H₂O), and a buffering acid (0.7 M H₃BO₃).^{11,13} Deposition was conducted at –1.2 V vs Ag/AgCl at room temperature. The currents increased quickly during the first 30 s and then became constant during deposition, indicating the ions are steadily diffused through the porous networks and deposited on the electrodes.

Sample Characterization. X-ray diffraction (XRD) patterns were recorded on a Siemens D-500 diffractometer using Cu K α

* Corresponding author. Phone: (504) 865-5827. Fax: (504) 865-6744. E-mail: ylu@tulane.edu.

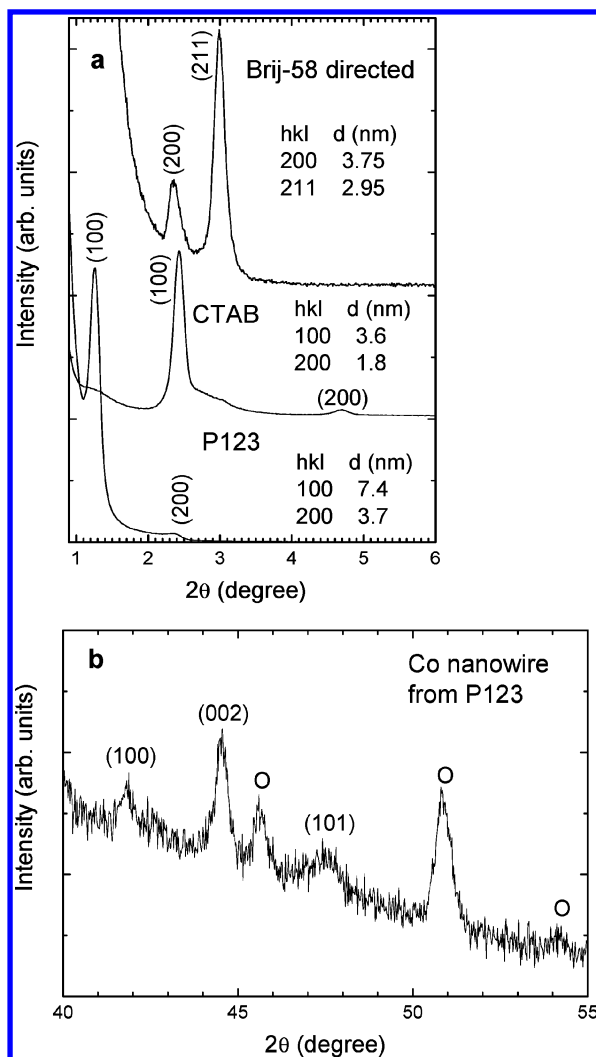


Figure 1. (a) Low-angle XRD patterns of the 2D hexagonal Co nanowire thin films directed from P123 and CTAB surfactant, and 3D cubic Co directed from Brij-58 surfactant, respectively. (b) Wide-angle XRD pattern of the Co nanowire thin film directed from P123 surfactant.

radiation. Transmission electron microscopy (TEM) images and selective area electron diffraction (SAED) patterns were obtained on a JEOL 2010 TEM microscope equipped with Oxford Link ISIS 6498 spectrometer for energy-dispersive X-ray (EDX) analysis and operated at 200 kV. The samples for TEM were prepared by scraping off the thin films from ITO-glass and directly placing them onto a carbon-coated copper grid. Magnetic characterization was carried out using the MPMS Quantum design superconducting quantum interference device magnetometer SQUID. The measurements were conducted using an applied field parallel or perpendicular to the film plane at room temperature. The bulk Co thin films were deposited on an Au sputtered Si wafer with a Cr adhesion layer.

Results and Discussion

The growth of the nanowires is initiated from the bottom conductive electrodes. Metal precursors, such as the cobalt ions, are continuously diffused through the porous channels and deposited on the electrodes. Such a bottom-up growing process gradually fills the pore channels of the templates with magnetic cobalt, resulting in the formation of continuously macroscopic nanowire thin films.³⁷ Through controlling the mesostructure of the mesoporous templates, cobalt nanowire thin films with the replicated mesostructure can be easily achieved. For

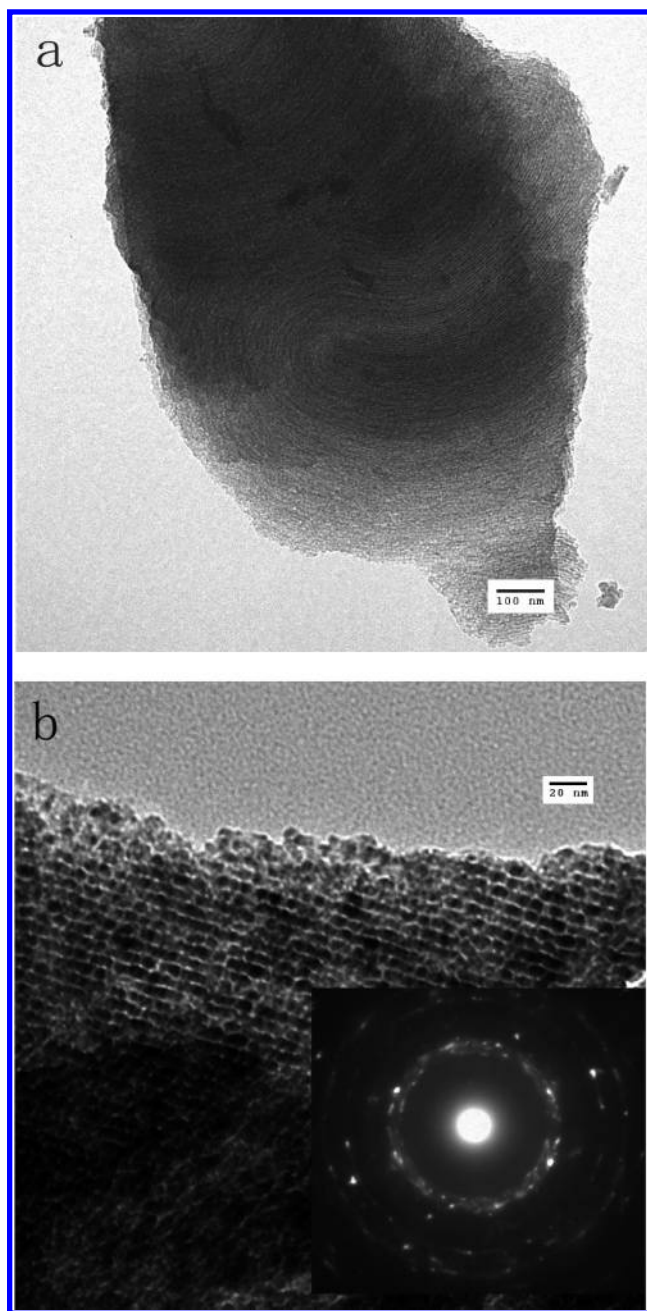


Figure 2. TEM images of (a) 2D hexagonal Co nanowire/silica directed from P123 surfactant and (b) 3D Co nanowire/silica directed from Brij-58 surfactant. Inset: SAED pattern of the Co nanowires showing the polycrystalline nature of the nanowires.

example, the use of mesoporous silica templates with 2D hexagonal or 3D cubic pore channels results in the formation of 2D nanowires or 3D nanowire networks, respectively.³⁷

Figure 1a shows the low-angle XRD patterns of Co nanowire thin films prepared using P123, CTAB, and Brij-58 directed mesoporous silica templates. The P123 directed Co nanowire thin film shows a typical 2D hexagonal structure with an intense (100) diffraction at the d spacing of 7.4 nm and a (200) diffraction at 3.7 nm. The CTAB directed Co nanowire thin film shows a similar 2D hexagonal structure with a (100) diffraction at the d spacing of 3.6 nm and a (200) diffraction at 1.8 nm. The absence of (110) diffraction for the 2D hexagonal structure of mesoporous silica is due to preferred orientation of the pore channels parallel to the film plane.²⁹ However, such hexagonal pore channels may form a swirling mesostructure due to the low bending energy of the surfactant tubules and the

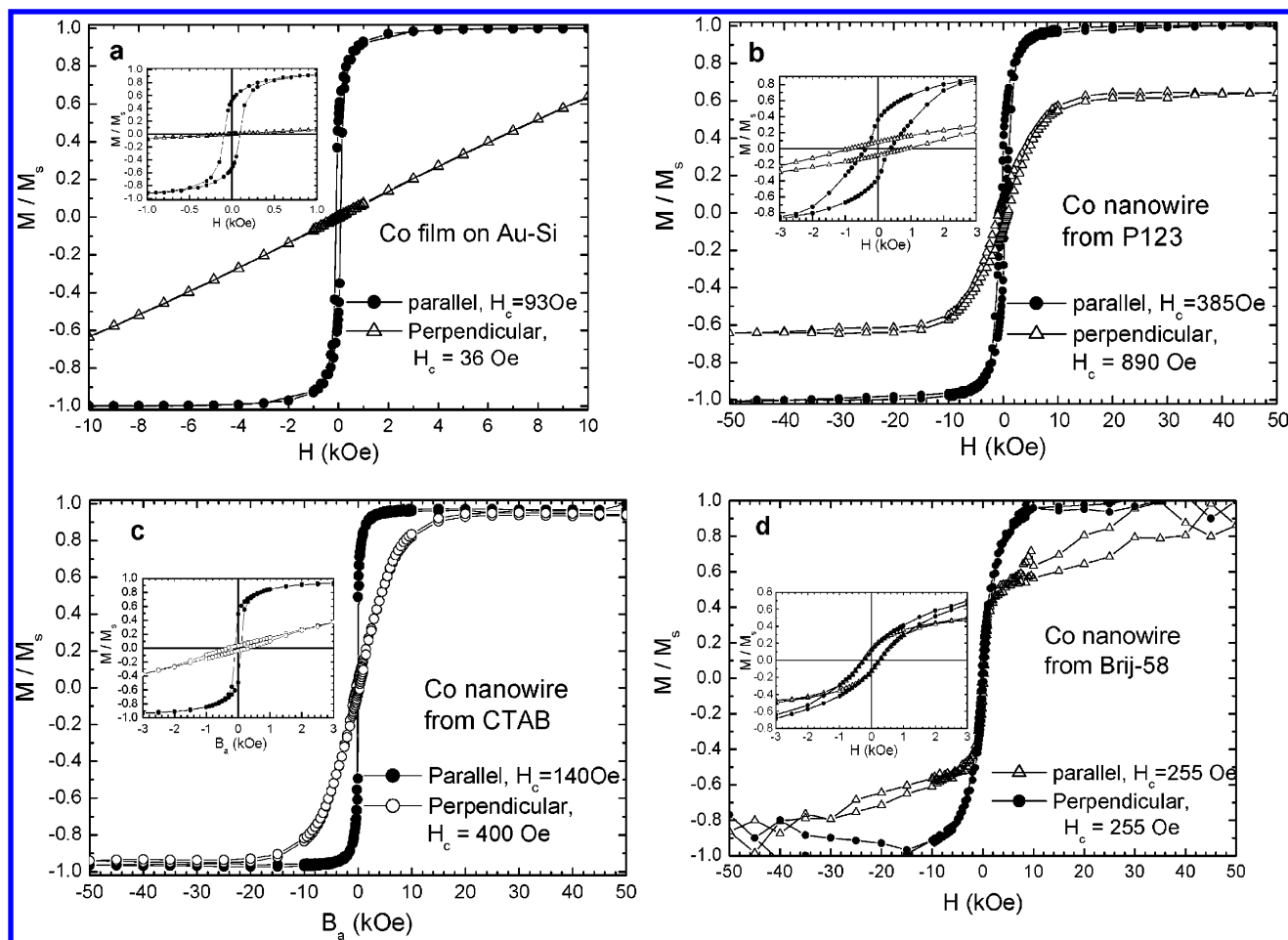


Figure 3. Room-temperature magnetic hysteresis loops of (a) Co film on Au–Si; (b) 2D Co nanowire thin film directed from P123 surfactant; (c) 2D Co nanowire thin film directed from CTAB surfactant; and (d) 3D Co nanowire thin film directed from Brij-58 surfactant.

inability of the liquid–vapor interface to impose long-range order on the tubule assembly process, which allows the transport of Co ions into the electrodes. The Brij-58-directed Co nanowire film shows a 3D cubic mesostructure with a (200) and (211) diffraction at the d spacing of 3.75 and 2.95 nm, respectively. Figure 1b shows a representative wide-angle XRD pattern of the P123 directed Co nanowire thin film. Except for the ITO substrate peaks (marked as o), the cobalt (100), (002), and (101) hcp diffraction peaks indicate a crystalline structure.

Figure 2 shows the TEM images of (a) the 2D hexagonal Co nanowires/silica directed from P123 surfactant and (b) the 3D Co nanowires/silica directed from Brij-58 surfactant. The inset SAED pattern indicates the polycrystalline nature of Co nanowires, which is consistent with the wide-angle XRD pattern. Figure 2a clearly shows the formation of nanowires swirling within the silica template. Figure 2b shows the formation of ordered Co nanowire arrays along the [111] direction of the cubic mesostructure. The average nanowire diameters are roughly equal to the average pore diameters of the templates, which are about 3, 5, and 8 nm, when CTAB, Brij-58, and P123 are respectively used as the pore structure directing agents.^{29–37}

Figure 3 shows the room-temperature magnetization hysteresis loops of (a) a bulk Co thin film, and (b) a Co nanowire film prepared using P123, (c) CTAB, and (d) Brij-58 directing agents. Comparison of the magnetization hysteresis loops clearly suggests that the mesostructure of the nanowires significantly affects the magnetic isotropy. As shown above, 2D nanowire thin films directed from P123 or CTAB surfactants possess nanowires that are preferably oriented parallel to the substrate

plane. Similar to the Co bulk thin film (a), such a shape anisotropy results in uniaxial anisotropic magnetism (b,c). As compared to the anisotropic 2D hexagonal mesostructure, the isotropic 3D cubic Co nanowire thin film shows isotropic magnetism (d). Although the magnetic signal is a little noisy, the inset of Figure 3d clearly shows approximately equal coercivity and remanent magnetization, which further confirms the pure cubic structure formation.

The nanostructure endows the nanowire thin films (b–d) with enhanced coercivity, as compared to the bulk Co film (a) that shows a low coercivity on the order of 10 Oe.^{11,13} As shown in Figure 3, the CTAB directed 3 nm Co nanowire thin film shows a parallel coercivity of 140 Oe and a perpendicular coercivity of 400 Oe. The Brij-58 directed 5 nm Co nanowire thin film shows an identical parallel and perpendicular coercivity of 255 Oe. The P123 directed 8 nm Co nanowire thin film shows a parallel coercivity of 385 Oe and a perpendicular coercivity of 890 Oe. It is well known that the coercivity of nanowires strongly depends on the wire diameters. The CTAB and P123 directed nanowire thin films contain similar 2D hexagonal mesostructure but different nanowire diameters. As shown above, the P123 directed nanowires (8 nm diameter) show a higher coercivity than the CTAB directed nanowires (3 nm diameter). As we mentioned before, the most nanowires investigated so far have diameters greater than 30 nm; the coercivity increased with decreasing wire diameters. Only Zeng et al. reported the magnetic properties of Fe, Co, and Ni nanowires with diameters between 9 and 21 nm, and they found the coercivity is closely related to the wire diameters and there

exists a maximum coercivity at 13 nm Fe, 10 nm Co, and 18 nm Ni, respectively.¹⁸ However, there is only one data point (9 nm) for Co nanowires below 10 nm. We present here the magnetic properties of Co nanowires with diameters as small as 3–8 nm. The 3 nm Co nanowires still show ferromagnetic behavior at room temperature due to the volume effect and enhanced magnetic shape anisotropy, instead of the superparamagnetism for 3 nm Co nanoparticles.^{1–3,9} This research for the first time demonstrates the room-temperature ferromagnetic behavior for Co nanowires with diameter as small as 3 nm. Note that this approach can be extended to prepare intermetallic CoPt and FePt nanowire thin films with intrinsically higher coercivities. A higher coercivity is a key factor for high-density information storage, although real devices also require intensive studies on surface roughness, local magnetization reversal characterization, and magnetization interaction, and other important issues. Nevertheless, such novel macroscopic magnetic nanowire thin films are of potential interest for high-density information storage application.

Conclusions

Using 2D and 3D mesoporous silica as templates, Co nanowire thin films with 3–10 nm diameters have been electrodeposited. They show ferromagnetic behavior at room temperature and exhibit higher coercivities as compared to bulk Co films. 2D nanowires show magnetic anisotropy and 3D nanowires show isotropy with identical coercivities and remanent magnetization on the parallel and perpendicular directions due to the shape effect.

Acknowledgment. This work was supported by NASA (Grant No. NAG-1-02070 and NCC-3-946), the office of Naval Research, the Louisiana Board of Regents (Grant No. LEQSF (2001-04)-RD-B-09), and the National Science Foundation (NSF-DMR-0124765, NER and CAREER award).

References and Notes

- Sellmyer, D. J.; Zheng, M.; Skomski, R. *J. Phys.: Condens. Matter* **2001**, *13*, R433.
- Fert, A.; Piroux, L. *J. Magn. Magn. Mater.* **1999**, *200*, 338.
- Martin, J. I.; Noguees, J.; Liu, K.; Vicent, J. L.; Schuller, I. K. *J. Magn. Magn. Mater.* **2003**, *256*, 449.
- Lederman, M.; O'Barr, R.; Schultz, S. *Trans. Magn.* **1995**, *31*, 3793.
- Dinega, D. P.; Bawendi, M. G. *Angew. Chem., Int. Ed.* **1999**, *38*, 1788.
- Chen, J. P.; Lee, K. M.; Sorensen, C. M.; Klabunde, K. J.; Hadjipanayis, G. C. *J. Appl. Phys.* **1994**, *10*, 5876.
- Sun, S. H.; Murray, C. B. *J. Appl. Phys.* **1999**, *85*, 4325. Sun, S. H.; Murray, C. B.; Weller, D.; Folks, L.; Moser, A. *Science* **2000**, *287*, 1989. Black, C. T.; Murray, C. B.; Sandstrom, R. L.; Sun, S. H. *Science* **2000**, *290*, 1131.
- Petit, C.; Taleb, A.; Pileni, M.-P. *Adv. Mater.* **1998**, *10*, 259; *J. Phys. Chem. B* **1999**, *103*, 1805.
- Puntes, V. F.; Krishnam, K. M.; Alivisatos, A. P. *Science* **2001**, *291*, 2115.
- Khan, H. R.; Loebich, O.; Rauscher, G. *Thin Solid Films* **1996**, *275*, 207. Khan, H. R.; Petrikowski, K. *J. Magn. Magn. Mater.* **2002**, *249*, 458.
- Xia, Y.; Yang, P.; Sun, Y.; Wu, Y.; Mayers, B.; Gates, B.; Yin, Y.; Kim, F.; Yan, H. *Adv. Mater.* **2003**, *15*, 370.
- Whitney, T. M.; Jiang, J. S.; Searson, P. C.; Chien, C. L. *Science* **1993**, *261*, 1316.
- Martine, C. R. *Science* **1994**, *266*, 196. Masuda, H.; Fukuda, K. *Science* **1995**, *268*, 1466.
- Thurn-Albrecht, T.; Schotter, J.; Kästle, G. A.; Emlay, N.; Shibuchi, T.; Krusin-Elbaum, L.; Guarini, K.; Black, C. T.; Tuominen, M. T.; Russell, T. P. *Science* **2000**, *290*, 2126.
- Ferré, R.; Ounadjela, K.; George, J. M.; Piroux, L.; Dubois, S. *Phys. Rev. B* **1997**, *56*, 14066.
- Ounadjela, K.; Ferré, R.; Louail, L.; George, J. M.; Maurice, J. L.; Piroux, L.; Dubois, S. *J. Appl. Phys.* **1997**, *81*, 5455.
- García, J. M.; Asenjo, A.; Velázquez, J.; García, D.; Vázquez, M.; Aranda, P.; Ruiz-Hitzky, E. *J. Appl. Phys.* **1999**, *85*, 5480.
- Sun, L.; Searson, P. C.; Chien, C. L. *J. Phys. Lett.* **1999**, *74*, 2803; **2001**, *79*, 4429. Chien, C. L.; Sun, L.; Tanase, M.; Bauer, L. A.; Hultgren, A.; Silevitch, D. M.; Meyer, G. J.; Searson, P. C.; Reich, D. H. *J. Magn. Magn. Mater.* **2002**, *249*, 146.
- Zeng, H.; Zheng, M.; Skomski, R.; Sellmyer, D. J.; Liu, Y.; Menon, L.; Bandyopadhyay, S. *J. Appl. Phys.* **2000**, *87*, 4718. Zheng, M.; Menon, L.; Zeng, H.; Liu, Y.; Bandyopadhyay, S.; Kirby, R. D.; Sellmyer, D. J. *Phys. Rev. B* **2000**, *62*, 12282. Zeng, H.; Skomski, R.; Menon, L.; Liu, Y.; Bandyopadhyay, S.; Sellmyer, D. J. *Phys. Rev. B* **2002**, *65*, 134426.
- Valizadeh, S.; George, J. M.; Leisner, P.; Hultman, L. *Electrochim. Acta* **2001**, *47*, 865.
- Yin, A. J.; Li, J.; Jian, W.; Bennett, A. J.; Xu, J. M. *J. Phys. Lett.* **2001**, *79*, 1039.
- Niensch, K.; Müller, F.; Li, A.-P.; Gösele, U. *Adv. Mater.* **2000**, *12*, 582. Niensch, K.; Wehrspohn, R. B.; Barthel, J.; Kirschner, J.; Gösele, U.; Fisher, S. F.; Kronmüller, H. *J. Phys. Lett.* **2001**, *79*, 1360.
- Ge, S. H.; Li, C.; Ma, X.; Li, W.; Xi, L.; Li, C. X. *J. Appl. Phys.* **2001**, *90*, 509. Ge, S. H.; Ma, X.; Li, C.; Li, W. *J. Magn. Magn. Mater.* **2001**, *226*, 1867.
- Cao, H. Q.; Xu, Z.; Sang, H.; Sheng, D.; Tie, C. Y. *Adv. Mater.* **2001**, *13*, 121. Cao, H. Q.; Tie, C. Y.; Xu, Z.; Hong, J. M.; Sang, H. *J. Phys. Lett.* **2001**, *78*, 1592.
- Han, G. C.; Zong, B. Y.; Wu, Y. H. *IEEE Trans. Magn.* **2002**, *38*, 2562. Han, G. C.; Zong, B. Y.; Luo, P.; Wu, Y. H. *J. Appl. Phys.* **2003**, *93*, 9202.
- Peng, Y.; Zhang, H. L.; Pan, S. L.; Li, H. L. *J. Appl. Phys.* **2000**, *87*, 7405. Peng, Y.; Shen, T.-H.; Ashworth, B. *J. Appl. Phys.* **2003**, *93*, 7050.
- Chu, S.-Z.; Wada, K.; Inoue, S.; Todoroki, S. *Chem. Mater.* **2002**, *14*, 4595.
- Zhang, X. Y.; Wen, G. H.; Chan, Y. F.; Zheng, R. K.; Zhang, X. X.; Wang, N. *J. Phys. Lett.* **2003**, *83*, 3341.
- Xue, K.-H.; Pan, G.-P.; Pan, M.-H.; Lu, M.; Wang, G.-H. *Superlattices Microstruct.* **2003**, *33*, 119.
- Lu, Y. F.; Ganguli, R.; Drewien, C.; Anderson, M.; Brinker, C. J.; Gong, W.; Guo, Y.; Soyey, H.; Dunn, B.; Huang, M.; Zink, J. *Nature* **1997**, *389*, 364.
- Zhao, D. Y.; Yang, P. D.; Melosh, N.; Feng, J. L.; Chmelka, B. F.; Stucky, G. D. *Adv. Mater.* **1998**, *10*, 1380. Alberius, P. C. A.; Frindell, K. L.; Hayward, R. C.; Kramer, E. J.; Stucky, G. D.; Chmelka, B. F. *Chem. Mater.* **2002**, *14*, 3284.
- Miyata, H.; Kuroda, K. *Chem. Mater.* **1999**, *11*, 1609.
- Han, Y.-J.; Kim, J. M.; Stucky, G. D. *Chem. Mater.* **2000**, *12*, 2068. Huang, M. H.; Choudrey, A.; Yang, P. D. *Chem. Commun.* **2000**, 1063.
- Gao, F.; Lu, Q. Y.; Liu, X. Y.; Yan, Y. S.; Zhao, D. Y. *Nano Lett.* **2001**, *1*, 743.
- Zhang, Z. T.; Dai, S.; Blom, D. A.; Shen, J. *Chem. Mater.* **2002**, *14*, 965. Zhang, Z. T.; Pan, Z. W.; Mahurin, S. M.; Dai, S. *Chem. Commun.* **2003**, 2584.
- Gross, A. F.; Diehl, M. P.; Beverly, K. C.; Richman, E. K.; Tolbert, S. H. *J. Phys. Chem. B* **2003**, *107*, 5475.
- Crowley, T. A.; Ziegler, K. J.; Lyons, D. M.; Ertz, D.; Olin, H.; Morris, M. A.; Holmes, J. D. *Chem. Mater.* **2003**, *15*, 3518.
- Wang, D. H.; Zhou, W. L.; McCaughy, B. F.; Hampsey, J. E.; Ji, X. L.; Jiang, Y.-B.; Xu, H. F.; Tang, J. K.; Schmehl, R. H.; O'Connor, C.; Brinker, C. J.; Lu, Y. F. *Adv. Mater.* **2003**, *15*, 130. Wang, D. H.; Luo, H. M.; Kou, R.; Gil, M. P.; Xiao, S. G.; Golub, V. O.; Yang, Z. Z.; Brinker, C. J.; Lu, Y. F. *Angew. Chem., Int. Ed.* **2004**, *43*, 6169.
- Pradhan, B. K.; Kyotani, T.; Tomita, A. *Chem. Commun.* **1999**, 1317.
- Knez, M.; Bittner, A. M.; Boes, F.; Wege, C.; Jeske, H.; Maiss, E.; Kern, K. *Nano Lett.* **2003**, *3*, 1079. Pradhan, B. K.; Kyotani, T.; Tomita, A. *Chem. Commun.* **1999**, 1317.